Towards Building Low Power Magnetic Communication Protocols for Challenging Environments

Amitangshu Pal, Rajpreet Kaur Gulati and Krishna Kant
Computer and Information Sciences, Temple University, Philadelphia, PA 19122
E-mail:{amitangshu.pal,rajpreet.gulati,kkant}@temple.edu

***Abstract*—Magnetic Induction (MI) based communication is a near-field communications technology that can work reliably in a variety of difficult propagation media and thus can be useful in many short-range IoT applications. In this paper, we explore low-power protocols for MI communications with low data rate requirements but a premium on energy consumption. In particular, we exploit *communication through silence* (CTS), and show that it can reduce the energy expenditure of the communication by up to 67% as opposed to typical binary packet based transmission. We also discuss a multi-channel tree based routing protocol to reduce energy consumption from *overhearing* in asynchronous MI communication networks and show that the proposed scheme can reduce the overhearing counts by ~60% with 2 channels and by ~80% with 4 channels.**

***Index Terms*—Magnetic induction communications, low-power MAC, multi-channel communication, experimental evaluations.**

I. Introduction

Smart sensing and wireless communication is a crucial element for infusing intelligence into a large variety of physical infrastructures. Radio frequency (RF) based communications are well established and cover a wide range of applications. For example, BlueTooth and related technologies are routinely used in personal area networks (PAN), whereas WiFi covers larger local area network (LAN) applications. More recently, IEEE has also defined a body area network (BAN) protocol, known as 802.15.6 [1] intended to have a short range (10-15m), very low power, high reliability, and high security.

These and most other RF protocols are intended to operate in the air, and thus may not be suitable for emerging IoT applications involving other types of media. For example, monitoring of the plant root systems in smart agriculture requires communication through the soil with varying degrees of organic matter, water, rocks, minerals,etc. The same holds for monitoring of leaks in water and sewer systems, online monitoring of quality and contamination in the fresh food supply chain, monitoring cluttered environment in industrial IoT, etc. RF based communication is generally quite challenging in all these environments. Aqueous media such as fresh food, soil organic matter, etc. absorb RF, particularly in the presence of salinity and metallic clutter causes diffraction and shadowing of RF signals. Furthermore, highly heterogeneous media such as underground operation that results in an extremely complex communications channel. Ultrasound is another well-established technology that works well in aqueous and underground media, but requires larger size radios and higher power consumption, but still cannot operate in a cluttered environment.

This research was supported by the NSF grant CNS-1844944 .

Because of these limitations, we have been exploring the magnetic induction-based communication that is reported to be much more effective in challenging environments [2]. MI communication is based on the principle of resonant inductive coupling (RIC), which involves two matched coils, each forming a LC circuit with the same resonance frequency. MI modulates the magnetic field and forms the basis of near field communications (NFC) between MI devices. MI does not involve propagating electromagnetic (EM) waves; instead, the varying magnetic field created by the transmit coil induces varying current in the receiver coil. This has very different characteristics than EM radiation.

The MI induction does not suffer from fading, and diffraction/absorption is generally expected to be much lower than RF. A key parameter for MI behavior is the magnetic permeability of the media, which is close that for the air for most materials including water, organic soil matter, fresh food, human body, non-ferrous metals (e.g., Aluminium), etc. MI radios can also be built to consume very low power. On the other hand, the range of MI is rather limited, both because of its faster decay than RF and because of the NFC nature (as discussed later). On balance, the technology is most appropriate for low data rate communications in environments where low power consumption is crucial.

Recognizing this potential of MI communications, IEEE has issued the 1902.1 standard in 2009 called RuBee operating at low frequency range of 30-900 KHz [3]. RuBee tags are basically coils with a non-volatile tag and a low power transmit circuitry that can be powered by the induced current in the coil. The few commercially available products include audio headphones by NXP [4] and Freelinc [5] MI radios, which operate at 13.56 MHz.

In this paper our primary objective is to develop low-power adaptive protocols for multi-hop MI communication networks. We assume a data-gathering tree/forest architecture where each sensor device collects and sends its packets to a centralized sink node. In this context, our main contributions are as follows. First, we use a *Communication Through Silence (CTS)* for low-power magnetic communication. Second, we discuss the issues of network *overhearing* for asynchronous MI communication networks and develop a *Joint Routing and Channel Selection (JRCS)* scheme to alleviate the overhearing effects. Finally through extensive simulations we show that the JRCS scheme can reduce the overhearing effects by ~60% with 2 channels and ~80% with 4 channels, whereas the CTS scheme can reduce the energy usage of the sensor nodes by upto 67% as opposed to packet based communication. We also

978-1-7281-1856-7/19/$31.00 ©2019 IEEE

show some experimental results on MI communication using a pair of off-the-shelf Freelinc radios.

The outline of the paper is as follows. Section II provides a brief overview of the MI communications including its applications and some experimental results. In section III we introduce our scheme of MI communication using silence duration as opposed to packet based communication. Section IV discusses the problems of overhearing in asynchronous, dense MI communication environments and introduces the multi-channel communication scheme to alleviate this. Related works are discussed in section V. We conclude the paper in section VI.

II. Overview of MI Communications

A. MI Communication Principles

Consider a pair of transmit and receiver magnetic coils, with K_t and K_r turns and a radii of ρ_t and ρ_r, respectively separated by distance r. Suppose that the coils are immersed in a media with permeability of μ ($\mu = 1$ for air, and close to 1 for most non ferromagnetic materials including metals). Consider the line segment formed by connecting the centers of the two coils. For a perfect induction, both coils should be perpendicular to this line. If not, the relative angles between them, say, θ_t and θ_r determine the induced magnetic flux between them, denoted as $F_{t\rightarrow r}$. It the transmit coil has current I_t flowing through it, then it can be shown that [6]

$$F_{t\rightarrow r} \approx I_t \frac{\mu\pi K_t K_r \rho_t^2 \rho_r^2}{2r^3} \left| \cos\theta_t \cos\theta_r - \frac{1}{2}\sin\theta_t \sin\theta_r \right| \quad (1)$$

The induced voltage is proportional to the rate of change of the magnetic flux (Lenz's Law). Therefore, the induced AC current will be the flux in equation (1) multiplied by the frequency of the transmitter current. It is seen that the radius of the coil (ρ_t and ρ_r) have a strong influence on the induced field, and the number of turns (K_t and K_r) also have proportional influence. This coupled with very rapid decay of the induced field with distance r means that (a) the technology is inherently a small range, and (b) to increase range, one must increase the size of coils and/or number of turns, both of which may be undesirable in applications where small size is required. The frequency and the transmit coil current directly increase the induced current, and hence the overall power consumption as well as the communication range.

The induction is a near-field phenomenon that applies for distances less than $\lambda/2\pi$ where λ is the wavelength of the transmit side current. The induced magnetic field decays very rapidly with distance r (as r^{-6}) in the near-field, which further limits the range of MI communications substantially. Fig. 1 shows the signal propagation of MI communication at 13.56 MHz. At 13.56 MHz the crossover point between the near and far field occurs at $\lambda/2\pi \approx 3.52$ meters. Thus when the communication range is smaller than 3.52 meters the signals decays at a rate of 60 dB per decade, whereas beyond this points it decades at 20 dB per decade. Similarly for 131 kHz (typically used for RuBee tags) the crossover points occurs at around 364 meters, however due to limited power and coil sizes the typical transmission range is only few tens of meters. The cosine law for energy transfer in MI ensures that 3 orthogonal coils can be stitched together to create a near isotropic transmission. Notice that in a tri-directional coil, the orthogonal coils on the same wireless device do not interfere with each other since the magnetic flux generated by one coil becomes zero at the other two orthogonal coils. A big advantage of isotropic pattern is that the coils deployed within a field do not need to be aligned identically with respect to one-another or the anchor coils. However, the isotropicity increases the form factor and requires coils oriented in each of the 3 dimensions.

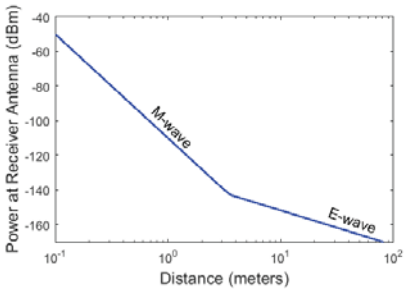

Fig. 1: MI Propagation at 13.56 MHz.

B. Applications of MI communications

As alluded to in the introduction, there are several applications where MI communications can provide a better solution than RF. In the following we briefly mention some of these.

Fresh Food Transportation and Distribution: Transportation and distribution (T&D) of fresh food is a huge and growing enterprise due to world wide sourcing of products, but it not only suffers from significant spoilage and waste, but also from dismal *efficiency*, which refers to the actual product carried by the T&D system as a fraction of its carrying capacity [7]. End to end quality and contamination tracking of the fresh food in the T&D pipeline has the potential to significantly reduce the food waste while improving the contamination tracking [8]. Radio frequency (RF) communications, although most popular, are unsuitable for such environments involving aqueous and animal/plant tissue media, dense environments (e.g., small regions with many radios), applications requiring extremely low power consumption, etc. For such environments, magnetic induction (MI) communications are an emerging technology that appears to be very attractive [9], [10].

Underground Soil Monitoring: Controlled use of fertilizers are important for plant growth and crop productivity. Automated sensing of soil nutrients like Nitrogen, Potassium, pH are important in applying the optimal supply of fertilizers at different places of the agricultural ground. However, embedding these sensors along with the radios underground brings a numerous challenges. As the RF communication does not penetrate through the ground and rocks, we can use MI transceivers to build this underground sensor network [11].

Underwater sensor networks: The applications of underwater WSNs (UWSNs) have huge potential for monitoring the health of marine aquaculture, underwater pollution detection and control, underwater habitat monitoring, climate monitoring and tracking any disturbances etc. UWSNs are also useful for oil or mining industries for oil/gas extraction, oil spills,

mine detection etc. Such networks can also be useful for monitoring underwater disasters such as underwater volcanic eruptions, underwater earthquakes that results in tsunamis, floods etc. Like underground environments, RF communication is also affected in UWSNs and thus using MI communications can be a feasible options for such environments [12].

C. Some Experimental Results

Although MI communications have been studied extensively in recent past, most studies involve either simulations or experiments that use the MI antenna (tuned LC circuits) driven by USRP boards. Because of the unavailability of commercial MI boards, it is difficult to truly validate the assertions made above. We have been working with Freelinc Inc [5] in this regard who have developed experimental but very well tuned MI boards for their R&D into MI. We were able to obtain two of these boards and interface each of them to a microcontroller (ARM7 based LPC2148) to conduct some experiments. This microcontroller is rather low-end (40 KB of on-chip static RAM and 512 KB of on-chip flash memory) but adequate run simple software for building and sending small packets to do throughput tests in various environments. The Freelinc radios operate on 13.56 MHz, with a current consumption of approximately 18mA. The Freelinc transmitter broad is equipped with 3-axis magnetic coils to provide near-isotropic transmission. Each of these coils uses a ferrite core, which helps enhance the transmission range considerably. The transmit coils have a diameter of < 5 mm with 5 turns, which allows for a reasonably small form factor. The receiver only has a single, flat rectangular coils without ferrite core, and thus is noticeably smaller.

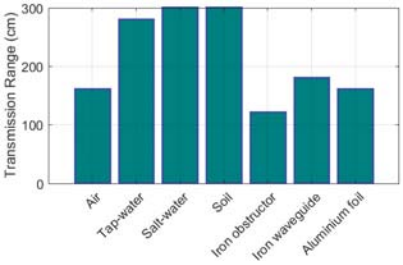

Fig. 2: MI transmission range with different media.

Fig. 2 shows the transmission range of MI transceivers in presence of different medias. We have conducted these experiments in a hallway. We have observed that in free space the transmission range is ~1.6 meters. To measure the transmission range of these MI transceivers in different mediums, we fill up few boxes with tap-water, salt water and soil and keep the them side-by-side to imitate the underwater and underground environment. We keep the transceivers at the opposite ends of these boxes to measure their transmission range. We have observed that with tap-water the transmission range is about 2.8 meters, whereas with salt water (with salt concentration of 33.4 gm/L) the range increases to ~3 meters. The transmission range in soil medium is also close to 3 meters, which is pretty similar to that of water.

We also place an iron plate in between the transceivers to observe its effect. We have observed that putting an iron plate in between reduces the transmission range to ~1.2 meters. On the other hand using the iron plate as an waveguide enhances the to ~1.8 meters. This is because an iron plate essentially acts like a mirror which "reflects" the magnetic flux and strengthen the signal [9]. We next covered the transceivers with aluminum foil to see its impact. We have observed that unlike RF communications the aluminum foil does not impact the MI transmissions and thus the transmission range remains the same as that of free space. More details of our experimental evaluations are reported in [13].

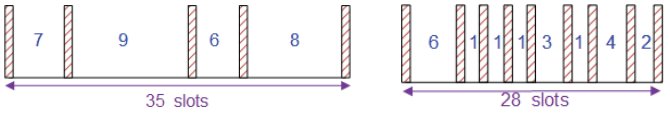

(a) (b)
Fig. 3: (a) Basic and (b) sorted CTS schemes.

However the existing transceiver pair is limited in many ways: (a) it has fixed operating frequency (13.56 MHz), which means that channel characterization at different frequencies, and dynamic channel switching is not possible, (b) inability to measure the induced current, received signal strength and path loss at the receiver, (c) inability to put the radios to sleep dynamically to explore low-power communication and networking etc. Thus in the following sections we have solely relied on simulation results to evaluate the proposed adaptations.

III. Low-Power Physical Layer Protocols

A. CTS: A Communication Scheme Through Silence

To enable the nodes with ultra low-power communication framework, we adopt a communication scheme through silence (CTS) [14]. The scheme relies on the time interval between two signals (in terms of number of clock ticks) to convey the required information. For example, if node n_1 wants to transmit the number X to n_2, it first sends a *start* symbol (or preamble) and then waits for X clock ticks before sending the *stop* symbol. Node n_2 starts its clock upon receiving the start signal and counts until it receives the stop signal in order to determine the sent value X. Of course, X needs to be limited to some maximum value, say, 2^m for some m, so that the mechanism effectively transfers m bits at a time. Longer packets could then be transmitted by sending an intermediate symbol after each m bit chunk. For example, Fig. 3(a) shows the transmission of (hexadecimal) 7968 using 4 bit chunks. We assume that the 3 symbols (start, stop, intermediate) are distinct and can be easily recognized by the receiver.

Such a mechanism saves energy than the normal binary scheme for several reasons. First, the number of actual symbol transmissions is reduced by a factor of m. Second, the transmitter can go to low power mode in-between symbol transmissions, particularly for the longer silence periods. Third, although the receive needs to count continuously, the receive circuitry can go to low power mode and woken up by the arrival of the next symbol. We will discuss these aspects later in detail.

However the improvement in energy comes at the cost of significantly increased delay and potentially time synchronization issues. The delay increases exponentially with m (as 2^m)

which means that m must stay rather small. This delay can be reduced by sorting the chunks and sending differences only. We call this as **sorted-CTS** approach, and is similar to the differential coding [15]. In our example, the string 7968 will be sorted to get 6789 and then transmitted as 6111, i.e., the smallest number followed by the successive differences. Obviously, the receive needs to know the original order in this case; therefore, we also need to send the order as well. Since we have four numbers in the packet, the ordering a permutation of the sequence 1234, namely 3142 (i.e., 3rd number is transmitted first, then first, then fourth, and then second). We again use the same basic silence mechanism to transmit these.

Fig. 3(b) shows the resulting transmission. The sorted scheme sends a total of 9 symbols with a total duration of 28 slots, as compared to 5 symbols with a total duration of 35 slots for the unsorted scheme. In effect, the delay is reduced at the cost of extra symbol transmissions. Obviously, there are cases where the sorted scheme will increase both the number of symbols and total duration, but generally it helps (as discussed later).

We now further discuss the choice of chunk size. With a chunk size of m, the maximum inter-symbol delay is 2^m and a packet of length L bits would need transmission of $N = L/m$ chunks. With $m = 6$ and a maximum packet size of 96 bytes, the packet transmission will require transmitting $N = 128$ chunks. A large m would not only cause large delays but is also undesirable from the clock integrity perspective. For example, if the slot duration varies by 0.1% due multipath or other effects, $m = 10$ could lead to incorrect slot counting on the receiver side. However for the short range communication (typical for MI) the delay spread due to multipath effects are usually small, and rarely exceed a few hundred nanoseconds [16]. Also MI communication is less affected by multipath propagation and thus is more robust the implementation of the CTS scheme. Also, the clock drifts for a maximum gap of 64 silence slots can be at most few nanoseconds and thus is negligible.

The mechanism requires an initial handshake between transmitter and receiver to agree to the essential parameters such as: (a) scheme type: sorted or not, (b) chunk size m, (c) maximum packet size N, and (d) slot size Δ (which determines the transmission rate). These could be either configured statically, or conveyed at the beginning of each session via normal binary transmission. The latter would require a PHY mechanism to distinguish between binary and silence based transmission. Such a capability could be useful in its own right – binary transmission when latency is important, and silence transmission when energy consumption is more important. However, we do not discuss the binary option from on.

We assume that each node has its own signal patterns, so that multiple nodes can transmit in parallel without interfering as far as their signals are not transmitted within the same slot. This would require establishing some maximum number of signal patterns at design time. If a collision is detected or a packet is received in error at the receiver, a NACK packet is sent. Upon reception of a NACK packet, the entire packet is re transmitted after a random waiting time. Since the CTS mechanism sends signals with a minimum of one slot gap, the receiver can send the NACK immediately after a signal collision is detected. This would avoid unnecessary continuation of corrupted packet. It is also possible that the collision is not recognized by the receiver either due to destructive interference or the collided symbols being considered as noise. In this case, the receiver will continue as normal. Additional mechanisms are then required to detect the corruption. The simplest possibility is to rely on the MAC level error checking using a mechanism such as CRC. It may also be useful to maintain a count of the number of chunks received before the end-packet signal.

B. Performance Evaluation

We now compare the performance of the proposed scheme against the normal binary transmission in terms of energy expenditure, packet latency, packet error rate and the probability of successful transmission.

Comparison of energy expenditure and delay: Regardless of the protocol, each packet starts with a preamble that allows the receiver detect the beginning of the frame. The preamble usually consists of a multiple bit pattern so that it is unlikely to be confused with packet contents. To avoid making the results specific to a chosen preamble length, we discount it from consideration in the following. Other than the preamble, the simple packet transmission needs L symbols for transmitting a packet with a value of at most 2^L. Thus the number of active slots $\mathcal{E}^{\mathrm{P}}$ (which is proportional to the energy expenditure) and packet latency $\mathcal{D}^{\mathrm{P}}$ is given by:

$$\mathcal{E}^{\mathrm{P}} = \mathcal{D}^{\mathrm{P}} = L \tag{2}$$

In the simple-CTS approach, the total worst case duration for a packet transmission with a value of 2^L is given by $L/m + 2^m L/m$. The first term is the transmitted bit duration, whereas the second term is for the worst case silence duration. This is because the worst case silence duration can be utmost 2^m duration in between a single digit. Thus the number of active slots $\mathcal{E}^{\mathrm{CTS}}$ and packet latency $\mathcal{D}^{\mathrm{CTS}}$ are

$$\mathcal{E}^{\mathrm{CTS}} = L/m, \qquad \mathcal{D}^{\mathrm{CTS}} = L/m + 2^m L/m \tag{3}$$

In the case of sorted-CTS the largest element of the digits can be utmost $2^m - 1$. Thus, regardless of the gaps between successive symbols, the total silence duration cannot exceed 2^m. In this case the number of active slots $\mathcal{E}^{\mathrm{sort-CTS}}$ and packet transmission delay $\mathcal{D}^{\mathrm{sort-CTS}}$ are given by:

$$\mathcal{E}^{\mathrm{sort-CTS}} = L/m + L/m \tag{4}$$

$$\mathcal{D}^{\mathrm{sort-CTS}} = L/m + 2^m + L/m + \sum_{i=1}^{L/m} i \tag{5}$$

The energy consumption can be viewed as consisting of two parts: (a) E_L, the energy required for the lowest level of radio operation that includes generation of the symbols, generation of gap, power amplification, and antenna energizing, and (b) E_H, the energy consumption due to higher level functions such as buffering a packet for transmission (or receiving a packet),

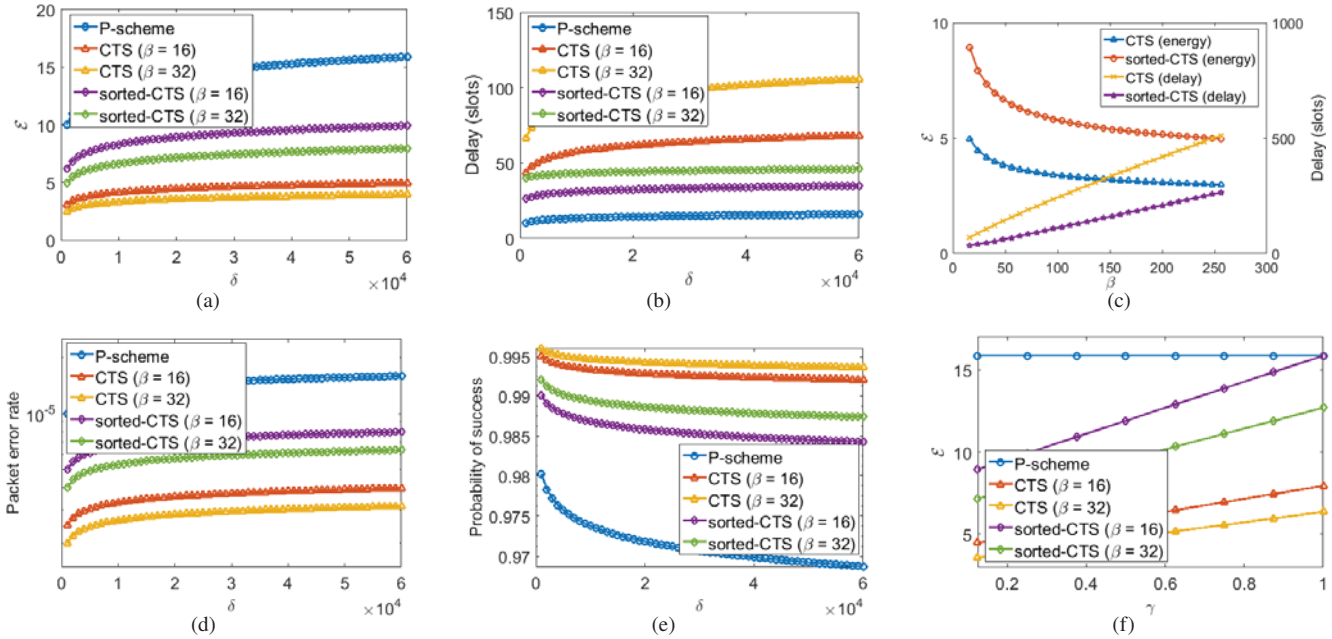

Fig. 4: Comparison of (a) transmitted energy, (b) delay performance, (c) Energy-delay trade off vs. 2^m, (d) Packet error rate, (e) Transmission success probability, (f) Transmission schemes with different γ.

clocking, beacon mechanism for discovery, association, and perhaps transmission scheduling (if any), collision detection and re-transmission, CRC calculation and checking, etc. Since E_H is mostly Phy independent, we will ignore it here. We also express $E_L = \mathcal{E}\xi$ where $\mathcal{E}$ is number of active transmission slots, and ξ is the energy required per slot. Obviously, ξ depends on the desired transmit power and the communication range we want to cover. As stated earlier, the magnetic communications are intended for short duration, and thus this part will be much smaller than, say, in a Bluetooth or other comparable RF radio. For communications in the range of a few meters, ξ is expected to be in a few μJ range.

The CTS scheme can save energy by putting the transmission mechanism of the radio into low-power (or sleep) mode after transmission of each symbol. The normal transmission mechanism will also make use of the sleep mode, but it will be entered only after the complete packet transmission. Each transition into and out of the sleep mode itself consumes energy, which we express as a fraction (say, γ) of the symbol transmission energy $\mathcal{E}$. We assume that the sleep mode energy consumption is negligible, which means that the per-symbol transmission energy is given by $(1+\gamma)\mathcal{E}$ units. We also assume that the transition time into and out of sleep mode are small enough so that the entire process of waking up, transmitting a symbol, and going to sleep can be comfortably accomplished within the same slot.

Fig. 4 shows the performance under various situations and comparison against the "P-scheme", or the simple binary packet transmission protocol. In these figures $\delta = 2^L$ and $\beta = 2^m$. comparison of energy expenditure $\mathcal{E}$ (which is $\mathcal{E}^{\text{P}}$, $\mathcal{E}^{\text{CTS}}$ and $\mathcal{E}^{\text{sort-CTS}}$ for three schemes respectively) and the packet latency for different protocols. Here we assume $\gamma = 1/4$. As expected the energy expenditure of CTS and sorted-CTS schemes are much lower than that of the packet based transmissions. From Fig. 4(a) we can observe that the CTS scheme reduces the energy expenditure by ~60% with $2^m = 16$. Increasing 2^m to 32 reduces the energy expenditure by upto ~67%. The sorted-CTS scheme almost doubles the energy consumption compared to the CTS scheme because of sending the additional signals for the order of the packet digits. However the energy consumption is still ~30-40% smaller than that of the normal packet transmission scheme.

The cost of the CTS scheme is the extra delay which is shown in Fig. 4(b). From this figure we can observe that the CTS scheme increases the delay by ~5-7 times. However the packet latency reduces drastically in case of sorted-CTS scheme, especially with increased 2^m. In fact as the packet length (i.e. 2^L) increases, the latency becomes ~2-3 times that of normal packet transmission scheme.

Fig. 4(c) shows the variation of energy consumption and delay with different 2^m. From this figure we can observe that the energy starts reducing with the increase in 2^m due to less number of signals transmitted. However the cost is extra delay due to higher gaps.

Comparison of packet error rate and probability of successful transmission: For binary transmission, the packet error probability consists of two elements: (a) framing error, resulting from start-of-packet and end-of-packet symbols not being recognized, and (b) packet content error caused by individual bits being flipped. Assuming similar preamble, (a) would be identical for both traditional and CTS schemes, and we will ignore it. With CTS, there are two additional factors: (c) variable delay in symbol arrival at the receiver which makes the receiver miscount the silence slots, and (d) noise during the silence period misconstrued as a symbol transmission. There are two potential sources for factor (c): (1) multipath signal spread which shifts the main lobe, and

(2) queuing delays at the transmitter when it handles multiple channels. Multipath delay spread is usually negligible over short distances that we are targeting here [16]. The queuing delays can be managed by ensuring that the number of channels and their utilization does not shift any transmission by more than 1/2 slot.

With a bit error rate of p_e, the packet error rate for binary transmission is given by

$$\mathcal{P}^{\mathrm{P}} = 1-(1-p_e)^L \tag{6}$$

This is because the packet is erroneous if any one of the bits is in error. Using the CTS scheme also results in higher packet success rate because of the transmission of fewer bits. For example assume that original message has L bits. The packet error probability of simple-CTS and sorted-CTS schemes are given by

$$\mathcal{P}^{\mathrm{CTS}} = 1-(1-p_e)^{L/m} \tag{7}$$

$$\mathcal{P}^{\mathrm{sort-CTS}} = 1-(1-p_e)^{L/m+L/m} \tag{8}$$

The probability of successful transmission also improves significantly in case of CTS scheme. Assume that the packets arrive at the nodes with a Poisson process at a rate of λ packet/slots. In presence of n such interferes, the probability of success of a test packet of L bits is given by

$$\gamma^{\mathrm{P}} = e^{-2n\lambda L} \tag{9}$$

This is because the vulnerable period in this scheme is given by $2L$ time units.

In case of CTS scheme, the total number of bits transmitted by a node is $\Upsilon_1 = L/m$. Assuming uniform distribution of the chunk values, the average gap between symbols for unsorted CTS scheme is 2^{m-1}. So we can assume that a node transmits $1/2^{m-1}$ symbols/slot while transmitting a packet. However, the transmission duration is also stretched by the same factor; i.e., the vulnerable period is $2(L/m)2^{m-1}$ slots. Thus the probability that none of the n interferes transmit during the vulnerable period is

$$\gamma^{\mathrm{CTS}} = e^{\frac{-2n\lambda(L/m)2^{m-1}}{2^{m-1}}} = e^{-2n\lambda(L/m)} = e^{-2n\lambda\Upsilon_1} \tag{10}$$

Similarly the packet success rate of the sorted-CTS scheme is given by

$$\gamma^{\mathrm{sort-CTS}} = e^{-2n\lambda\Upsilon_2} \tag{11}$$

where $\Upsilon_2 = 2L/m$; here the multiplier "2" results from the fact that the sorted-CTS sends the chunk order in addition to the actual data.

Fig. 4(d) shows the packet error rate of different schemes with bit error rate $p_e = 10^{-6}$. As we can observe that the CTS schemes can significantly reduce the packet error rate due to the reduced number of transmitted bits. On the other hand Fig. 4(e) shows the packet success probabilities of different schemes with $n = 10$ and $\lambda = 10^{-4}$ packets/slots. Because of transmitting the smaller number of bits, the CTS schemes drastically improves the packet success probability even with higher bit rates. The packet success probability of the sorted-CTS is less than the unsorted one as $\Upsilon_2 > \Upsilon_1$.

C. MIMO Communication for Increasing Data-rate

For increasing the data-rate of MI communication, it is possible to integrate six coils in one module by essentially combining two sets of 3 orthogonal coils. Fig. 5 shows two separate coil sets where the axes are at 45 degrees relative to one another. If two are put together (with proper isolation between them) but operate on different channels, it should be possible to have more compact sensor modules. These modules can send packets using these two sets of coils in parallel, which results in MIMO communication and can increase the transmission rate. However, such mechanisms can increase the rate by a factor of the number of channels and thus we ignore the details in this paper.

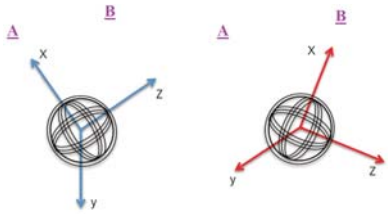

Fig. 5: Merging 2 orthogonal coils.

D. Few Notes On CTS-based communication

Even if the proposed CTS-based scheme reduces a significant amount of energy consumption, it has a some realistic concerns. First, is the additional energy for switching on/off the radios before/after the transmission of a signal. Thus the scheme is efficient for circuitry with very fast on/off capability. Fig. 4(f) shows the energy consumption of the nodes where γ is the fraction of the transmission energy consumption due to radio wake-up and putting it to sleep. From this figure we can observe that the energy consumption of the CTS schemes increase gradually with the increase in γ. In fact, the energy consumption of the sorted-CTS is almost identical to the traditional packet transmission with $2^m = 16$ and $\gamma = 1$. Thus the CTS scheme is best suited for higher 2^m and with lower radio on/off time. Second, the received message will be erroneous if the relative time difference between the signals are wrongly decoded. To ensure this, the duration of a time slot needs to be kept little above of a signal duration. Overall the CTS scheme incurs higher delay and is suitable for small packet sizes with low transmission rates. Third, the sorted-CTS scheme will incur additional delay and energy consumption due to sorting. Since the sorting is an integral part of packet transmission, we assume that the Phy layer does it in hardware. This would involve loading the contents of the packet buffer into a sorting network that implements parallel bitonic sort and outputs the result to another buffer. The number of items to be sorted is modest; e.g., 96 numbers, each 6-bits long for a 128 byte message. Assuming a sorting network built from Xilinx Virtex 7 like FPGA blocks [17], the cost of a synchronous, pipelined sorter can be expressed as [18]

$$n_{\mathrm{LUTs}} = 5m(p^2+p)2^{p-3}, \quad n_{\mathrm{FFs}} = 4m(p^2+p)2^{p-3} \tag{12}$$

where m is the number of bits, $p = \log_2 N$ (N is the number of items or chunks to be sorted), n_{LUTs} is the number of look up table operations (to implement combinational logic) and n_{FFs} is the number of bit store operations using flip-flops. (Note that these are number of operations, not the number of units

required). For $m = 6$ and $N = 128$, $p = 7$, and we need about 26.9K LUTs and 21.5K FFs. The number of stages in bitonic sort are $p(p+1)/2$, or 28. Assuming a latency of about 5 ns per stage (200 MHZ operation), we get 140 ns latency.

To get a ballpark estimate of the energy consumption, assume about 10 gates per LUT or FF. The dynamic power consumption of 32 nm process logic gate is reported to be about 120 FJ in [19]. It will likely decrease with smaller feature size, but the wire power (not accounted for) will likely go up. We conservatively assume 240 FJ/gate including the wires. This yields a dynamic energy consumption of about 115 nJ/packet. The static power consumption of a logic gate is about 8 pA [19], and we again double it to account for the wires. This yields 274 nA/stage/packet (the static power is consumed only by the active stage). Assuming operation at 1.0V, this corresponds to 274 nJ/packet. However, this large figure assumes that all gates are on all the time. Most chips will use aggressive power gating mechanisms to control static power consumption. Assuming only 30% of the gates are alive at any time, we have 82 nJ of static power per packet. With a packet rate of 1000 packets/sec, this corresponds to 115+82=197 μW total power consumption. Based on our earlier assumption, this is more than an order of magnitude lower than the transmit power and thus is ignored.

IV. Joint Multi-Channel Communication and Routing

A. A Low-Power MAC

We will integrate a low-power wake up mechanism shown in Fig. 6 to isolate the radio electronics from the coil. The wake up circuit is triggered by the induced current in the coil and wakes up the radio receiver electronics only when the induced current is above some threshold. By using this phenomenon, we propose a low-power asynchronous MAC protocol for near-field magnetic communication, which is shown in Fig. 7. To conserve energy, the nodes sleep most of the time and wake-up only at the time of transmission/reception. Before transmitting a packet, the transmitter listens to the channel. If the channel is idle, it transmits a short preamble before transmitting the actual data packet, which is sufficiently long to wake-up the receiver circuit. Due to the near-field transmissions via the coupled magnetic field, the receiver coil can detect the MI signal without actively listening.

Fig. 6: Wake-up circuit illustration.

However, due to such induction based wake-up and reception, all the nodes that are in the neighboring regions of the transmitter also receive the preamble and the data packets, which causes a serious *overhearing* problem especially in a dense environment. *Such overhearing problem becomes extremely severe in very dense sensing applications, which is quite unlike in the typical sensor network situation. The longer delay of the CTS scheme makes the situation even worse.*

Fig. 7: Low power MAC ("P": Preamble, "D": Data).

Fig. 8 shows the average current consumption of a sensor node under different node density. In Fig. 8, we assume that the beacon messages are transmitted once in 15 minutes. The current consumption due to transmission and reception are assumed to be of 20 mA, whereas the radios stay on for preamble and data transmissions for 140 milliseconds. From this figure we can observe that the current consumption increases *almost linearly* with the increase in neighbor density. This also motivates the necessity of reducing the effect of overhearing in such asynchronous multi-hop WSNs. Our objective is to design a *joint routing and channel selection (JRCS) scheme* to adapt the energy consumption in the nodes that are critically resource constrained, by *controlling their corresponding overhearing traffic*. In such a dense networks, interference is also a crucial issue, especially when more and more packages are going to be equipped with the sensing nodes. We address these issue through multichannel communications.

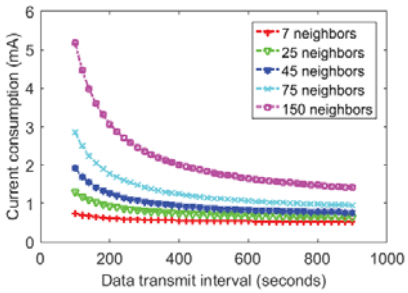

Fig. 8: Average current consumption vs. node density.

B. JRCS Protocol Overview

In order to reduce interference (and overhearing) due to involuntary induction of current in the coils, we propose to use multiple channels. Since the MI-based communication has a short transmission range, multihop communication becomes necessary when there is no direct link between a sensor device and its nearest anchor node. Hence, a data-gathering tree/forest needs to be constructed (or reconstructed) when the network is formed (or changed) so that each sensor device has a path to its nearest anchor node.

We thus propose a distributed and joint multihop routing and channel selection scheme for single-radio, asynchronous MI sensor networks which is explained as follows. We define the *receiver channel* of a node to be its designated channel for receiving all incoming packets. In contrast, a *transmit channel* is the one to which a node switches temporarily to transmit, and is the receiver channel of the intended destination. Nodes select their receiver channels to enable distribution of traffic over multiple orthogonal channels. Since nodes listen to their receiver channels by default, interference/overhearing is limited to neighboring transmissions on a node's receiver channel only.

In our scheme the nodes randomly choose a channel as its receiver channel. Also the nodes send beacon messages in different channels in rotation. This ensures that all their neighbors are able to receive the beacon messages within a bounded time, irrespective of their receiver channels. The bea-

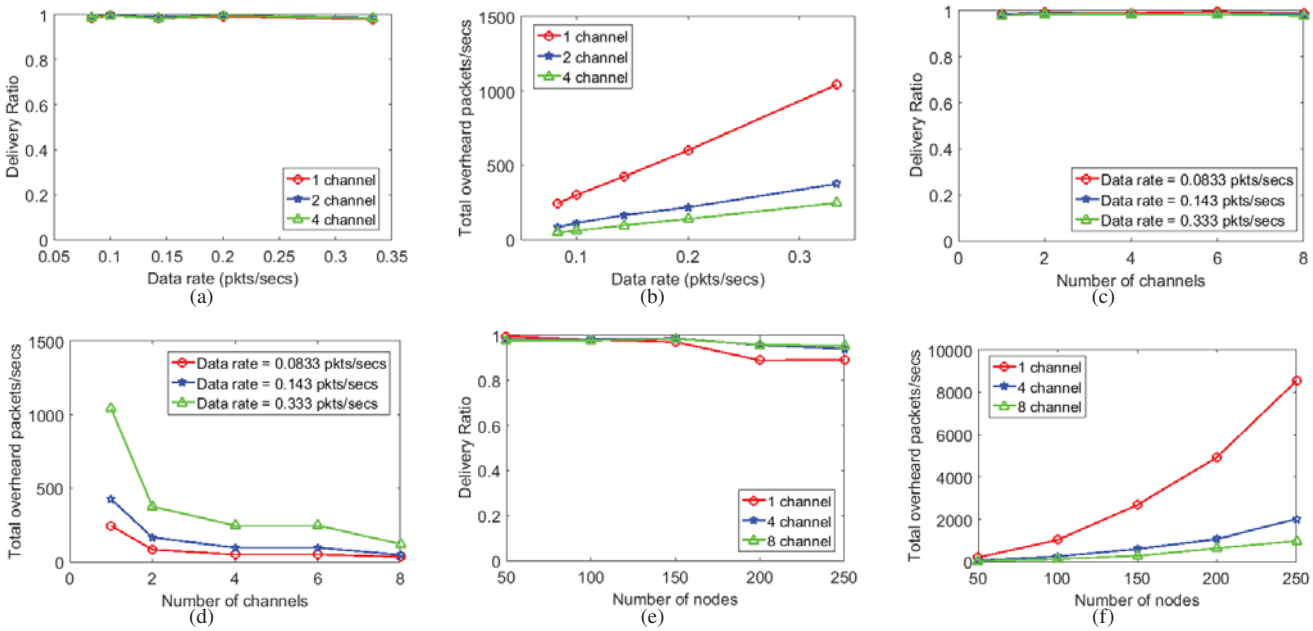

Fig. 9: Comparison of packet delivery ratios and packet overhearing with (a)-(b) different data rates, (c)-(d) number of channels and (e)-(f) node densities.

con messages carry the following fields: ⟨nodeID, its receiver channel, sequence number, path-metric⟩ where the path-metric is defined as follows. The path-metric and route selection is done similar to the collection tree protocol (CTP) [20]. We use a path metric that is obtained as the sum of the *expected number of transmissions (ETX)* on each of its links. An ETX for a link is the expected number of transmission attempts required to deliver a packet successfully over the link. In CTP, path selection is performed based on maximizing a path quality metric, which implies minimizing the path-ETX, which is the sum of link ETXs along the path. This is achieved as follows. The sink always broadcasts an ETX = 0. Each node calculates its ETX as the ETX of its parent plus the ETX of its link to the parent. This measure assumes that nodes use link-level acknowledgements and re-transmissions. A node i chooses node j as its parent among all its neighbors if

$$\text{ETX}_{ij}+\text{ETX of } j < \text{ETX}_{ik}+\text{ETX of } k \quad \forall k \neq j \qquad (13)$$

where ETX_{ij} and ETX_{ik} are the ETX of link $i \rightarrow j$ and $i \rightarrow k$ respectively. In this process a node chooses the route with the lowest ETX value to the sink.

Corresponding to each neighbor j, a node i records the following fields in its neighbor table: ⟨nodeID of j, receiver channel of j, ETX of j, link-ETX of $i \rightarrow j$⟩. This table is updated with the new ETX values, which is calculated based on which fraction of the beacon and/or data messages transmitted by node-j is received successfully at node-i. Thus whenever node-i sends a data packet to its parent (assume its parent is j), it temporarily switches to the receiver channel of j, complete the transmission and then return back to its own receiver channel. Routing loops and repairing happens similar to the CTP.

One potential drawback of the proposed scheme is the additional delay and power consumption of the *channel switching* at the time of transmissions. However in our applications the transmission are rather infrequent and so is the channel switching. Also, the additional delay and energy consumption for low-power RF radios are rather small [21] which we believe will apply to MI communications as well. The protocol also has no additional overhead other than periodic beacon message transmissions.

C. Performance Evaluation

We evaluate the performance of JRCS using *Castalia* simulator [22]. We place the sensor nodes in an area of 20×20 meter^2. For channel modeling we assume a log-normal shadowing model with path-loss exponent of 6, with a standard deviation of 4 dBm. The path loss at a reference distance 1 is assumed to be of 55 dBm. We assume additive interference model for our simulations. The transmit power is assumed to be of 0 dBm. We set the re-transmission limit to 30.

Comparison with different data-rates: Fig. 9(a)-(b) show the variation of packet delivery ratio and overhearing counts with different transmission rates. We assume that 100 nodes are placed uniformly in the geographic area. From this figure we can observe the overhearing counts is reduced by ~60% with the use of 2 channels and by ~80% with 4 channels. We can also observe that the packet delivery ratio does not vary significantly due to the channel switching in JRCS as observed from Fig. 9(a).

Comparison with different number of channels: Fig. 9(c)-(d) show the variation of packet delivery ratio and overhearing counts with different number of channels. We assume 100 nodes for this set of figures. From this figure we can observe that the overhearing reduces significantly with the increased number of channels, however *the improvement does not scale with the increasing in number of channels*. Notice that the receiver channel assignment is similar to the graph coloring problem; however, due to limited number of channels, it may not be possible to assign different channel to neighboring vertices. Now the graph coloring problem can be seen as

implicit set cover problem where the subsets consists of the independent sets (or non-neighboring vertices) of the graph. As the set cover problem can be formulated in terms of sub-modular functions[1] the effects of increasing the number of channels results in decreasing marginal utility, which is evident from Fig. 9(b)-(d).

Comparison with different network size: We next vary the network size by varying the number of sensor nodes from 50 to 250. The number of channels are chosen to be 4. We keep the data transmission rate per node as 0.333 packets/seconds. Fig. 9(e)-(f) show that the overhearing increases by ∼40-95 times while the number of sensor nodes increases from 50 to 250. This is because of the higher network density, which results in significant increase in overhearing. We can also observe an increase in packet delivery ratio (upto 7%) with increased number of channels as compared to the single channel scenario. This shows that even if the delivery ratio is not affected with low network density, it starts reducing as the network density grows which results in network interference. Thus the use of multiple orthogonal channels also reduces the level of network interference in highly dense MI communication environment and at the same time results in reduced network overhearing.

V. Related Work

Magnetic induction (MI) communication is first proposed as an alternative to Bluetooth technology in [23]. MI has been proposed for many environments including underwater [12], pipeline monitoring applications [24], food sensing and communication infrastructures [9], [10] etc.

As for developing low-power protocols in sensor network is well-mined. Several low-power MAC protocols are explored for controlling the sleep/wakeup cycle of the sensor radios [25]. Multi-channel communication schemes are also well-explored in wireless networks [26]. In the context of sensor networks several approaches are developed for assigning channels for sensor networks, such as tree-based channel assignment [27], control theory [28] or game-theory [29] based channel assignment etc. However these schemes are mostly focused on minimizing network interference. As opposed to that our scheme is developed for alleviating the overhearing effects caused by the neighboring transmissions of the sensor nodes.

VI. Conclusions

Near-field magnetic induction communication is an alternative to RF in applications where the communication is mainly unaffected by water, minerals, biological material, etc. In this paper, we developed and discussed new way of low-power adaptive protocols for building MI communication networks, including communication techniques through silence, low-power medium access scheme for MI communication and multi-channel tree formation protocol for data collection. We have also discussed a feasibility study of a magnetic communication experiment using Freelinc boards. As these boards are limited flexibility, we are currently developing MI modules that can switch between sleep-wake up cycles or choose their transmit power and channel dynamically. We also plan to conduct experiments in real application scenarios, including underground mediums, wearable body areas networks, etc.

[1] A set function $f : 2^{\mathcal{T}} \rightarrow \mathbb{R}$ is called sub-modular, if for every $\mathcal{A}, \mathcal{B} \subseteq \mathcal{T}$ with $\mathcal{A} \subseteq \mathcal{B}$ and every $x \in \mathcal{T} \setminus \mathcal{B}$ we have that $f(\mathcal{A} \cup \{x\}) - f(\mathcal{A}) \geq f(\mathcal{B} \cup \{x\}) - f(\mathcal{B})$.

References

[1] M. Ghamari *et al.*, "Comparison of low-power wireless communication technologies for wearable health-monitoring applications," in *I4CT Conf.*, April 2015, pp. 1–6.
[2] A. Pal and K. Kant, "NFMI: connectivity for short-range iot applications," *IEEE Computer*, vol. 52, no. 2, pp. 63–67, 2019.
[3] http://ru-bee.com/.
[4] "NXP Introduces Ultra-low Power Radio Transceiver Enabling Wireless Earbuds." [Online]. Available: https://www.nxp.com/products/wireless/miglo:NFMI-RADIO-SOLUTIONS
[5] "Freelinc," http://www.freelinc.com/.
[6] X. Tan and Z. Sun, "Environment-aware indoor localization using magnetic induction," in *IEEE GLOBECOM*, 2015, pp. 1–6.
[7] K. Kant and A. Pal, "Internet of perishable logistics," *IEEE Internet Computing*, vol. 21, no. 1, pp. 22–31, 2017.
[8] A. Pal and K. Kant, "Smart sensing, communication, and control in perishable food supply chain," 2019, submitted to ACM TOSN.
[9] A. Pal and K. Kant, "Magnetic induction based sensing and localization for fresh food logistics," in *IEEE LCN*, 2017, pp. 383–391.
[10] A. Pal and K. Kant, "Iot-based sensing and communications infrastructure for the fresh food supply chain," *IEEE Computer*, vol. 51, no. 2, pp. 76–80, 2018.
[11] Z. Sun and I. F. Akyildiz, "Magnetic induction communications for wireless underground sensor networks," *IEEE Transactions on Antennas and Propagation*, vol. 58, no. 7, pp. 2426–2435, 2010.
[12] I. F. Akyildiz *et al.*, "Realizing underwater communication through magnetic induction," *IEEE Communications Magazine*, vol. 53, no. 11, pp. 42–48, 2015.
[13] R. Gulati *et al.*, "Experimental evaluation of a near-field magnetic induction based communication system," in *IEEE WCNC*, 2019.
[14] Y. Zhu and R. Sivakumar, "Challenges: Communication through silence in wireless sensor networks," in *ACM MobiCom*, 2005, pp. 140–147.
[15] B. Krishnaswamy *et al.*, "Time-elapse communication: Bacterial communication on a microfluidic chip," *IEEE Trans. Communications*, vol. 61, no. 12, pp. 5139–5151, 2013.
[16] J. P. Linnartaz, "Jpl's wireless communication reference website," 2006. [Online]. Available: http://www.wirelesscommunication.nl/reference/chaptr03/fading/delayspr.htm
[17] X. Corp., "Virtex-7 T and XT FPGAs Data Sheet: DC and AC Switching Characteristics," 2017. [Online]. Available: https://www.xilinx.com/support/documentation/data_sheets/ds183_Virtex_7_Data_Sheet.pdf
[18] R. Mueller *et al.*, "Sorting networks on FPGAs," *The VLDB Journal*, vol. 21, no. 1, pp. 1–23, 2012.
[19] A. Wiltgen *et al.*, "Power consumption analysis in static cmos gates," in *SBCCI*, 2013, pp. 1–6.
[20] O. Gnawali *et al.*, "Collection tree protocol," in *SenSys*, 2009, pp. 1–14.
[21] A. Pal and A. Nasipuri, "A joint routing and channel assignment scheme for hybrid wireless-optical broadband-access networks," *Journal of Sensor and Actuator Networks*, vol. 7, no. 4, 2018.
[22] "Castalia: A Simulator for WSN," http://castalia.npc.nicta.com.au/.
[23] R. Bansal, "Near-field magnetic communication," *IEEE Antennas and Propagation Magazine*, vol. 46, no. 2, pp. 114–115, 2004.
[24] X. Tan *et al.*, "On localization for magnetic induction-based wireless sensor networks in pipeline environments," in *IEEE ICC*, 2015, pp. 2780–2785.
[25] Y. Kim *et al.*, "Y-MAC: An energy-efficient multi-channel mac protocol for dense wireless sensor networks," in *IPSN*, 2008, pp. 53–63.
[26] A. Pal and A. Nasipuri, "JRCA: A joint routing and channel assignment scheme for wireless mesh networks," in *IEEE IPCCC*, 2011.
[27] Y. Wu *et al.*, "Realistic and efficient multi-channel communications in wireless sensor networks," in *INFOCOM*, 2008, pp. 1193–1201.
[28] H. K. Le *et al.*, "A control theory approach to throughput optimization in multi-channel collection sensor networks," in *IPSN*, 2007, pp. 31–40.
[29] Q. Yu *et al.*, "Multi-channel assignment in wireless sensor networks: A game theoretic approach," in *INFOCOM*, 2010, pp. 1127–1135.